

# CNN deep learning-based monitoring of stress and damage using of electromechanical impedance responses of CSA sensor

JEONG-TAE KIM, QUOC-BAO TA, NGOC-LAN PHAM  
Department of Ocean Engineering  
Pukyong National University  
Busan, KOREA

**Abstract:** A multi-task 2D CNN model is designed for integrated monitoring stress and damage in concrete specimens utilizing the raw impedance signatures of capsule-like smart aggregated (CSA). The fundamental theory of CSA-based EMI method is presented to describe how the sensor responds to compressive loads. Next, compression tests on a CSA-embedded concrete cylinder are conducted to record the stress-damage EMI responses of CSA sensor under applied stresses. The multi-task 2D CNN model learned the impedance signals for predicting the concrete stress and damage is constructed. Consequently, the generalization and robustness of the developed model are tested against noise and untrained data.

**Keywords:** impedance-based, PZT sensor, capsule-like smart aggregate, convolutional neural network, stress estimation, damage identification.

Received: April 11, 2024. Revised: September 17, 2024. Accepted: November 19, 2024. Published: December 31, 2024.

## 1. Introduction

Concrete structures play a vital role in civil infrastructure due to their adaptability and cost-effectiveness. After a prolonged operation period, key components in concrete structures experience degradation and damage from continuous stress. In recent studies, the CNN-based regression algorithms have been integrated with EMI techniques for stress estimation of concrete structures. Nguyen et al. employed a 1D CNN algorithm to learn damage-sensitive EMI features for monitoring damage in prestressed concrete girders [1]. Ta et al. [2,3] developed an impedance-based 1D CNN regression model for stress monitoring in concrete using raw EMI data from SA and CSA sensors. The stress in the investigated concrete structure could be automatically estimated with high accuracy, even under noise effects and missing data. The mentioned works demonstrated the accuracy of the deep learning method in stress estimation in concrete structures even in the presence of noise and missing data.

CNN-based classification algorithms have also been integrated with EMI techniques for damage identification in concrete structures. An impedance-based 1D CNN deep learning approach was proposed to detect bolt loosening in steel structures using raw EMI data [4]. Another study by Nguyen et al. employed the 1D CNN model to detect damage in PZT transducers [5]. Yan et al. [6] proposed a 1D CNN integrated with EMI data to evaluate the early-age hydration of cement mortar, outperforming traditional machine learning methods in quantifying EMI response changes.

Despite previous research efforts, existing CNN deep learning models could handle stress estimation and damage detection tasks separately using either CNN-based regression or CNN-based classification. The status of the concrete structures under compression has not been fully explored. To address these gaps, this paper introduces a multi-task 2D CNN model that integrates regression and classification, enabling the simultaneous monitoring of concrete stress and damage using CSA-based EMI responses.

This study presents a multi-task 2D CNN model for integrated monitoring stress and damage in concrete specimens utilizing the raw impedance signatures of capsule-

like smart aggregated (CSA). The fundamental theory of CSA-based EMI method is presented to describe how the sensor responds to compressive loads. Next, compression tests on a CSA-embedded concrete cylinder are conducted to record the stress-damage EMI responses of the CSA sensor under applied stresses. The multi-task 2D CNN model learned the impedance signals for predicting the concrete stress and damage is constructed. Consequently, the generalization and robustness of the developed model are tested against noise and untrained data.

## 2. CSA-based EMI Measurement Technique

The CSA sensor prototype for the EMI measurement technique is shown in Fig. 1. The CSA sensor is fabricated by attaching a PZT patch onto an aluminium interface, which is covered by a hollow aluminium capsule. The dimensions of the CSA prototype are  $L \times W \times H = 25 \times 25 \times 11$  mm [7]. The aluminium interface plate considers the CSA capsule's wall as fixed ends protected and is allowed to vibrate freely. The thickness of 2 mm of vibrating plate is chosen to pre-determine the sensitive frequency band of the CSA sensor [8].

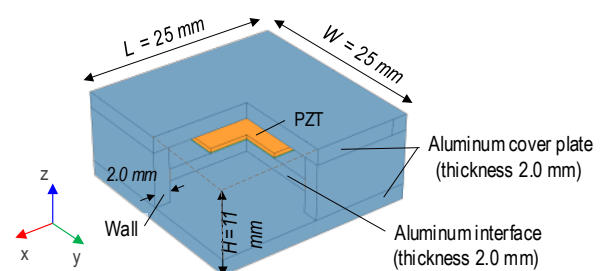


Fig. 1. Prototype of capsule-like smart aggregate (CSA)

Figure 2 shows a model of CSA-based impedance monitoring for concrete structures. When stress is applied, the CSA sensor embedded in the concrete structure experiences compressive stress ( $\sigma_N$ ) along with the vertical direction (i.e., z-direction). At the same time, the other CSA's surfaces (i.e., y-direction and x-direction) are subjected to tension stress ( $\sigma_T$ ) due to Poisson's effect (see Fig. 2a). As a result, the vibrating plate undergoes expansion under the tensile stress in both the

y-direction and x-direction. The CSA's deformation affects the structural state of the vibrating plate and impedance responses of the PZT attached to it (see Fig. 2b and 2c).

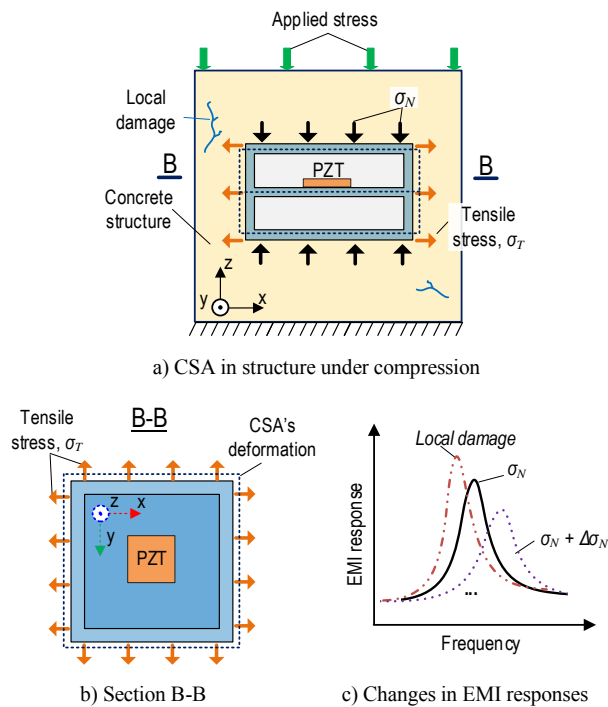


Fig. 2. Behavior of EMI responses of CSA embedded in concrete structure under applied stress in z-direction

When the applied stress (e.g.,  $\sigma_N + \Delta\sigma_N$ ) increases and reaches the yield condition of the concrete material, the local damage may occur. When the damage occurs, the tensile stress on the vibrating plate is released rapidly, leading to abrupt changes in the EMI responses [7,9], as shown in Fig. 2c.

### 3. Experimental Test

#### 3.1 Fabrication of CSA-Embedded Concrete Cylinder

Figure 3 presents the fabrication procedure for a CSA-embedded concrete cylinder. A CSA sensor was strategically placed in a cylinder mold measuring  $100 \times 200$  mm. The CSA was positioned 140 mm from the bottom of the cylinder mold. To secure the CSA sensor within the mold, plastic wires and a steel bar (2 mm in diameter and 150 mm in length) were utilized. After 28 days of the curing process, the concrete cylinder embedded with CSA sensor was used for the impedance test.

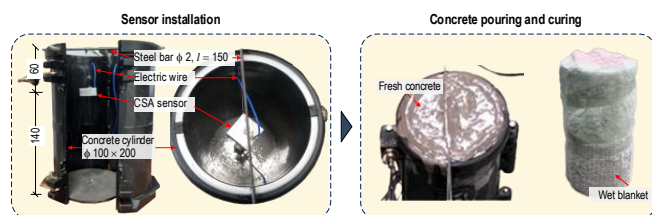


Fig. 3. Fabrication of CSA-embedded concrete cylinder

#### 3.2 Experimental Setup

The experimental setup for compression test of concrete cylinder is presented in Fig. 4. The MTS servo-hydraulic materials testing system (version 793) was employed for the compression test. The compression force of system was real-time monitored by a load cell with a capacity of up to 500 kN. An impedance analyzer (HIOKI 3532) was utilized to capture stress-damage EMI signals from the CSA sensor, while a KYOWA EDX-100A measured the ambient temperature.

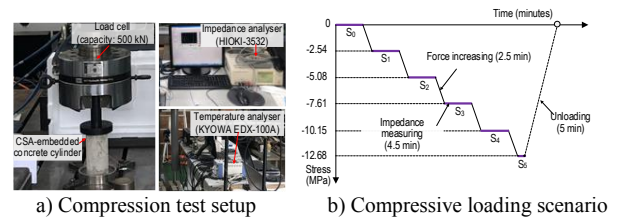


Fig. 4. Experimental setup for compression test of concrete cylinder

EMI responses were measured in frequency range of 15 kHz to 26 kHz using 224 intervals. The notable peaks in EMI responses in this range could be used to assess the sensitivity of the embedded CSA sensor to compressive loading. The recorded EMI responses, along with corresponding structural attributes (i.e., stress levels and concrete damage levels), were compiled to create a stress-damage EMI dataset for the 2D CNN deep regression and classification model. The measured temperature ranged between  $22^\circ\text{C}$  and  $23^\circ\text{C}$ . Due to the minor variation of  $1^\circ\text{C}$ , the temperature effect on the EMI responses was considered negligible.

Figure 4b shows six loading scenarios ( $S_0 = 0$  MPa to  $S_5 = 12.68$  MPa) introduced to the CSA-embedded cylinder. The stress was applied in constant increments of 2.54 MPa within 2.5 minutes, maintaining a consistent loading rate of 0.0113 MPa/s. Following each increment, the stress increment was paused for 4.5 minutes to obtain EMI responses.

#### 3.3 Stress-Damage EMI Signatures of CSA-Embedded Concrete Cylinder

Figure 5 plots the EMI responses collected in six stress levels (i.e.,  $S_0$  to  $S_5$ ). As the applied stress increased, both the frequency and magnitude of the resonant peak exhibited a downward trend. The variation in peak frequency and peak magnitude were potentially caused by the high compressive stress on the CSA sensors during concrete strength development. The corresponding visual observation of the test specimen under applied stresses  $S_0$ - $S_5$  is shown in Fig. 6. At loading level  $S_3$ , initial crack imitation was observed. As loading progressed to level  $S_4$ , crack propagation and concrete spalling were noted. Ultimately, concrete damage continued to develop, leading to failure at loading level  $S_5$ .

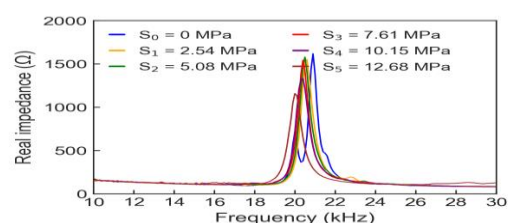


Fig. 5. Impedance responses of CSA sensor under  $S_0$ - $S_5$

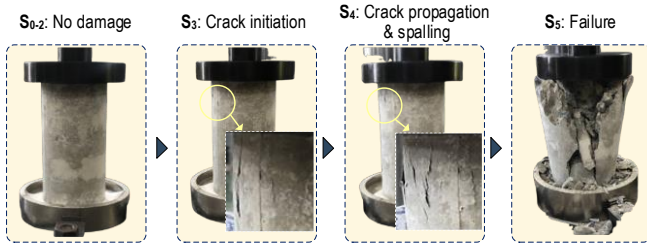


Fig. 6. Observer concrete damage of test specimen under  $S_0$ - $S_5$

## 4. Evaluation of Multi-task 2D CNN-based Deep Regression and Classification Model

### 4.1 Design of Multi-task 2D CNN Model

Figure 7 illustrates the architecture of a multi-task 2D CNN deep learning model using raw EMI responses of CSA sensor. The model employs regression learning for stress estimation and classification learning for damage identification in concrete structures. The parameters and hyperparameters of the model are selected based on previous studies [10,11] and practical guidelines [12].

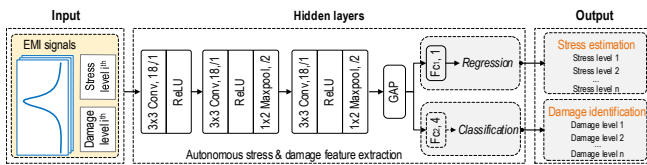


Fig. 7. Architecture of 2D CNN deep regression and classification model

The model includes three convolutional (Conv) layers, three ReLU layers, two Maxpool layers, a global average pooling (GAP) layer, two fully connected (Fc) layers, and separate Regression and Classification output layers. The multi-task 2D CNN model generates two outputs: "Stress estimation" handled by regression learning, and "Damage identification" handled by classification learning.

### 4.2 Stress and Damage Monitoring for Noise-Contaminated Stress-Damage EMI Data

#### 1) Data Preparation

The measured EMI data from the CSA-embedded concrete cylinder and corresponding assigned labels (i.e., "stress" and "damage level") is listed Table 1. The stress level  $S_0$  (0 MPa) was excluded from the model configuration due to the uncertainty in experimental measurements. For regression learning, compression forces ranging from 2.53 MPa to 12.68 MPa were labelled with five stress levels ( $S_1$  to  $S_5$ ). For classification learning, the damage severity of test specimen (i.e., "No damage," "Crack initiation," "Crack propagation and spalling," and "Failure") was labelled with four levels "DL0," "DL1," "DL2," and "DL3," respectively.

In the compressive test of concrete specimen, the EMI signals were measured with four ensembles for each applied stress level, resulting in a total of 20 signals across five stress levels. Gaussian noise was employed to enrich the databank and to investigate the generalization and robustness of the multi-task 2D CNN model on noise contamination. The

training dataset was generated by adding six Gaussian noise levels (0-5%) with four iterations to the first two ensembles at each stress level. It resulted in a total of 240 EMI signals generated for five applied stress levels. The third ensemble from each level was used to construct the validation set, which consisted of five EMI signals in total. Similar for the testing dataset, noise levels ranging from 1% to 5% (in 1% increments) were applied to the last ensemble, generating ten new EMI signals per stress level. This resulted in 250 additional EMI signals across all noise levels. Combined with the five original EMI signals, the testing dataset comprised a total of 255 signals. The validation set takes the third ensemble of data collected at each stress level, resulting in five signals in total.

TABLE I. ASSIGNED LABELS OF STRESS-DAMAGE EMI DATA FOR MULTI-TASK 2D CNN MODEL

Stress level	Observed concrete damage	Assigned label	
		Stress (MPa)	Damage level
$S_1$	No damage	2.53	DL0
$S_2$	No damage	5.07	DL0
$S_3$	Crack initiation	7.61	DL1
$S_4$	Crack propagation and spalling	10.15	DL2
$S_5$	Failure	12.68	DL3

The training set is visualized in Fig. 8. Each EMI signal was labelled with its corresponding stress level and damage status. With 225 data points for each EMI signal, a total of 10,800 data points were obtained for each stress level. For five stress levels, the total number of data points was 54,000. Examples of noise-contaminated stress-damage EMI signals are shown in Fig.9.

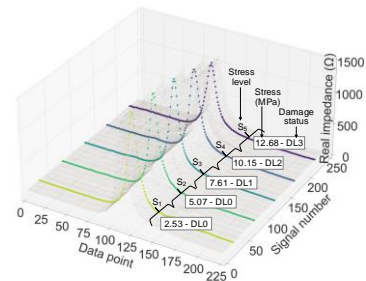


Fig. 8. Visualization of training set of multi-task 2D CNN model

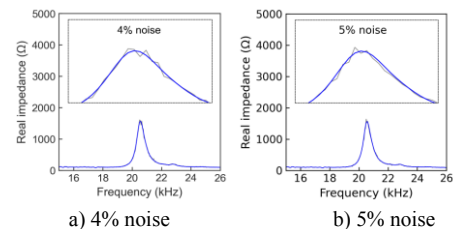


Fig. 9. Visualization of noise-contaminated EMI signals

#### 2) Training Results

Figure 10 plots the loss values of the 2D CNN model over 100 training epochs. Overall, both the training and validation losses showed fluctuations and generally followed a decreasing trend as training progressed. The 2D CNN model, consisting of 6,143 training parameters, required 35.1 seconds to complete the training process.

Figure 11 shows two representative results of investigating the effects of noises on the stress estimation and damage identification of the multi-task 2D CNN model. For stress estimation, the accuracy of the model decreased as the levels of noise increased. The relationship between the RMSE index and noise levels is illustrated in Figure 12a. For damage identification, the model maintained performance with no false predictions at noise levels up to 4%. Misclassifications began to occur at a noise level of 5%, leading to an increase in the false discovery rate to 2.5%, as shown in Figure 12b.

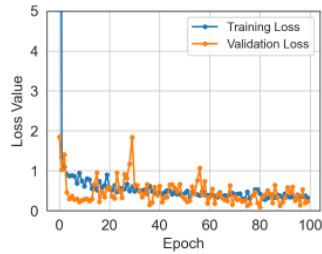


Fig. 10. Loss values of 2D CNN model after 100 epochs

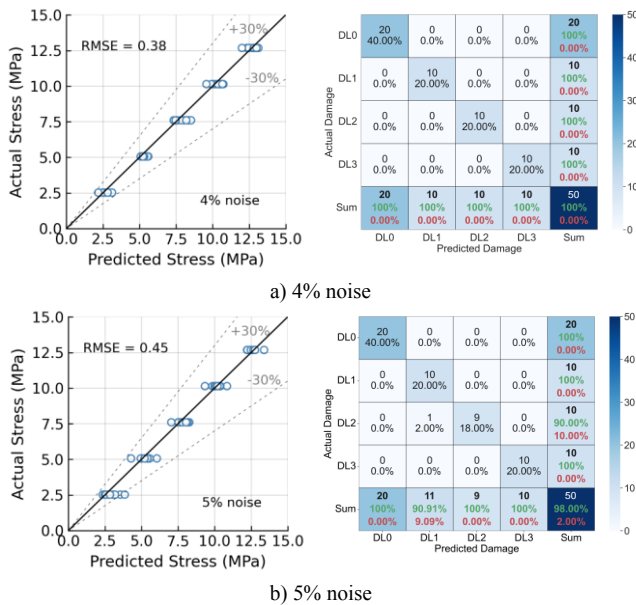


Fig. 11. Stress prediction and damage identification by 2D CNN model

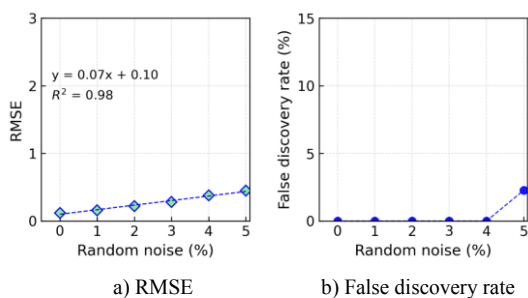


Fig. 12. Stress estimation and damage identification performance of 2D CNN model

### 4.3 Stress and Damage Monitoring for Untrained Stress-Damage EMI Data

#### 3) Data Preparation

To assess the performance of the multi-task 2D CNN model under missing data conditions, the EMI signals corresponding to stress level  $S_2$  were excluded from the training and validation sets. This led to the removal of 48 signals from the training set and one signal from the validation set. As a result, the training and validation sets consisted of 192 signals and four signals, respectively (see Fig. 13). The testing set had a total of 255 signals for five applied stress levels.

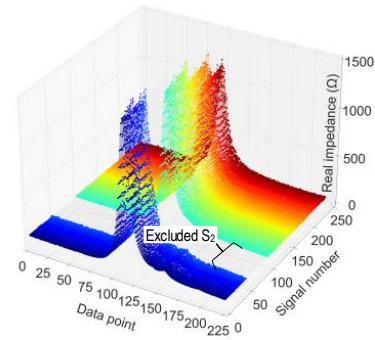


Fig. 13. Visualization of partial untrained training set for 2D CNN model

#### 4) Training Results

Figure 14 plots the training process of the multi-task 2D CNN model using the designed dataset. It is observed that the training loss gradually converged, while validation loss fluctuated during the whole training process (100th epoch).

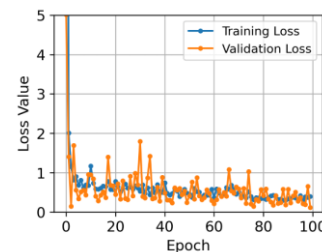


Fig. 14. Loss values of 2D CNN model with partial untrained databank

Figure 15 shows presentative results of stress estimation and damage identification with partial untrained databank. For stress estimation, the predicted stress levels showed consistency with actual stress, achieving an RMSE value of 0.57. The prediction error for the untrained stress level  $S_2$  was within 30% at a noise level of 5%. The relationship between RMSE and noise levels is shown in Fig. 16a, where RMSE values increased as noise levels increased. For damage identification, some misclassifications occurred for the partial untrained damage level DL0. The overall prediction accuracy was 84% at a noise level of 5%. The false discovery rate for damage identification across six noise levels is summarized in Fig. 16b.

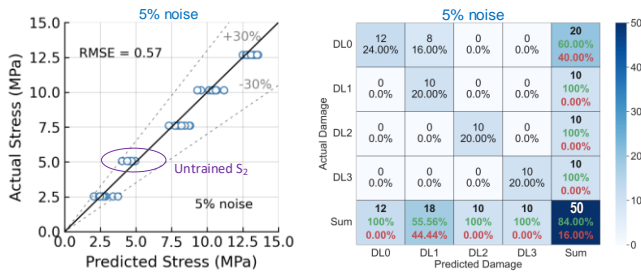


Fig. 15. Stress estimation and damage identification of 2D CNN model with partial untrained databank

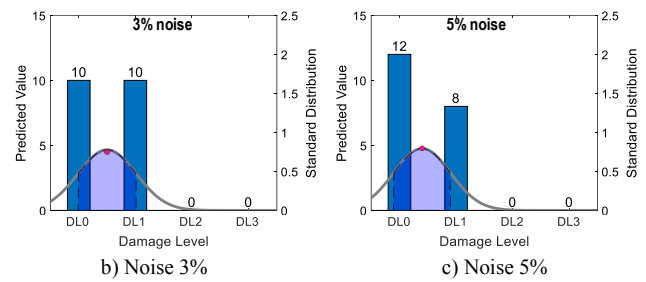


Fig. 17. Probability assessment of damage identification results with partial untrained databank

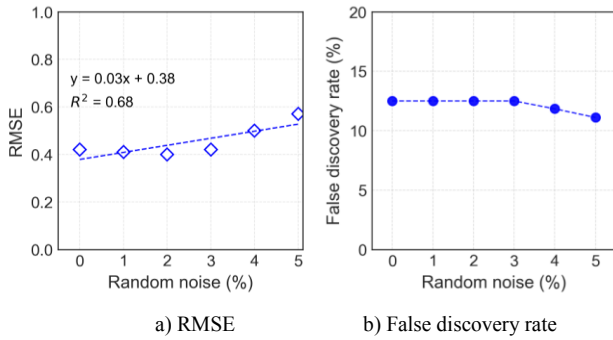
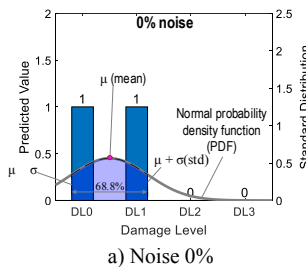


Fig. 16. Stress estimation and damage identification performance of 2D CNN model with partial untrained databank

### 5) Discussion on Damage Identification Results

Figure 17 shows the probability assessment of damage identification results of damage level "DL0" with partial untrained databank. A portion of "DL0" data, corresponding to stress level  $S_2$ , was excluded from the training and validation phases. The x-axis in the figure represents the four damage levels ("DL0"-"DL3"), while the left and right y-axes denote the predicted value and standard distribution, respectively.

The shaded area indicates the range within one standard deviation ( $\sigma$ ) from the mean ( $\mu$ ), encompassing 68.8% of the predicted values around the central tendency. For all three noise levels (i.e., 0%, 3%, and 5%), the shaded region indicated damage levels "DL0" and "DL1". The mean value was balanced between "DL0" and "DL1" at 0% and 3% noise levels, and it shifted toward "DL0" at noise level 5%.



## 5. Concluding Remarks

In this study, the multi-task 2D CNN model was developed for integrated monitoring stress and damage in concrete specimens utilizing the raw impedance signatures of capsule-like smart aggregated (CSA). The fundamental theory of CSA-based EMI method was presented to describe how the sensor responds to compressive loads. The compression tests on a CSA-embedded concrete cylinder were conducted to record the stress-damage EMI responses of CSA sensor under applied stresses. The multi-task 2D CNN model learned the impedance signals for predicting the concrete stress and damage was constructed. The generalization and robustness of the developed model were validated against noise and untrained data.

## Acknowledgment

This work was supported by the Basic Science Research Program through the National Research Foundation of Korea.

## References

- [1] Pham, Q.-Q., Ta, Q.-B., and Kim, J.-T., "Capsule-like Smart Aggregate with Pre-Determined Frequency Range for Impedance-Based Stress Monitoring," *Sensors*, vol. 23, no. 1, pp. 434, 2022.
- [2] Nguyen, T.-T., Ta, Q.-B., Ho, D.-D., Kim, J.-T., and Huynh, T.-C., "A method for automated bolt-loosening monitoring and assessment using impedance technique and deep learning," *Developments in the Built Environment*, vol.14, pp. 100122, 2023.
- [3] Nguyen, T.-T., Ho, D.-D., and Huynh, T.-C., "Electromechanical impedance-based prestress force prediction method using resonant frequency shifts and finite element modelling," *Developments in the Built Environment*, vol. 12, pp. 100089, 2022.
- [4] Ta, Q.-B., Pham, Q.-Q., Pham, N.-L., Huynh, T.-C., and Kim, J.-T., "Smart Aggregate-Based Concrete Stress Monitoring via 1D CNN Deep Learning of Raw Impedance Signals," *Structural Control and Health Monitoring*, vol. 2024, no. 1, pp. 25, 2024.
- [5] Ta, Q.-B., Pham, Q.-Q., Pham, N.-L., and Kim, J.-T., "Integrating the Capsule-like Smart Aggregate-Based EMI Technique with Deep Learning for Stress Assessment in Concrete," *Sensors*, vol. 24, no. 14, 2024.
- [6] Nguyen, T.-T., Kim, J.T., Ta, Q.B., Ho, D.D., Phan, T.T.V., and Huynh, T.C., "Deep learning-based functional assessment of piezoelectric-based smart interface under various degradations," *SMART STRUCTURES AND SYSTEMS*, vol. 28, no. 1, pp. 69-87, 2021.
- [7] Yan, Q., Liao, X., Zhang, C., Zhang, Y., Luo, S., and Zhang, D., "Intelligent monitoring and assessment on early-age hydration and setting of cement mortar through an EMI-integrated neural network," *Measurement*, vol. 203, pp. 111984, 2022.
- [8] Pham, Q.-Q., Ta, Q.-B., Park, J.-H., and Kim, J.-T., "Raspberry Pi Platform Wireless Sensor Node for Low-Frequency Impedance Responses of PZT Interface," *Sensors*, vol. 22, no. 24, 2022.

- [9] Kocherla, A., and Subramaniam, K.V.L. (2020), "Embedded smart PZT-based sensor for internal damage detection in concrete under applied compression," *Measurement*, Vol. 163.
- [10] Lecun, Y., Bottou, L., Bengio, Y., and Haffner, P., "Gradient-based learning applied to document recognition," *Proceedings of the IEEE*, vol. 86, no. 11, pp. 2278-2324, 1998.
- [11] Pham, N. L., Ta, Q. B., and Kim, J. T., "CNN-Based Damage Identification of Submerged Structure-Foundation System Using Vibration Data," *Applied Sciences*, vol. 14, no. 17, pp. 7508, 2024.
- [12] Zhang, Y., and Wallace, B., "A sensitivity analysis of (and practitioners' guide to) convolutional neural networks for sentence classification," *arXiv preprint arXiv:03820*, 2015

### **Contribution of Individual Authors to the Creation of a Scientific Article (Ghostwriting Policy)**

The authors equally contributed in the present research, at all stages from the formulation of the problem to the final findings and solution.

### **Sources of Funding for Research Presented in a Scientific Article or Scientific Article Itself**

No funding was received for conducting this study.

### **Conflict of Interest**

The authors have no conflicts of interest to declare that are relevant to the content of this article.

### **Creative Commons Attribution License 4.0 (Attribution 4.0 International, CC BY 4.0)**

This article is published under the terms of the Creative Commons Attribution License 4.0

[https://creativecommons.org/licenses/by/4.0/deed.en\\_US](https://creativecommons.org/licenses/by/4.0/deed.en_US)